Calculation of NMR Line Shapes Using the Memory-Function Approach

G. W. Parker and F. Lado
Department of Physics, North Carolina State University, Raleigh, North Carolina 27607
(Received 4 June 1973)

The formal solution of the line-shape problem in terms of a memory function has been used to illustrate the calculation of line shapes characteristic of both liquids and solids. A memory function is associated with a corresponding free-induction-decay (fid) curve and it is related to the behavior of a local-field correlation function. Its relaxation time T_2^{**} varies from a relatively large value in solids $T_2^{**} \approx M_2^{-1/2}$, to a very short value in liquids $T_2^{**} \ll M_2^{-1/2}$, where $M_2 = \langle \Delta\omega^2 \rangle$ is the second moment of the absorption line. In spite of this wide range of decay times the functional form of a memory function remains insensitive to the form of a line shape. This insensitivity may be exploited in the calculation of line shapes. The method requires a knowledge of the qualitative form of a line shape and the first few of its moments and is a compromise between a qualitative approach and a full miscroscopic calculation of the relevant spin autocorrelaton function. Examples discussed include pair line shapes in solids, line shapes during motional narrowing, exchange-narrowed line shapes in paramagnetic MnF_2, and fid curves in CaF_2.

I. INTRODUCTION

Since the pioneering work of Bloembergen, Purcell, and Pound, the characteristic line shapes of nuclear magnetic resonance have been recognized to be the Lorentzian and Gaussian curves.[1,2] The Lorentzian function is characteristic of narrow absorption lines in liquids and describes the effect of lifetime broadening on the states of an individual spin interacting with the rapidly fluctuating magnetic field produced by its neighbors.[1-3] More generally, this function is obtained as a solution of the Bloch equations.[4] The Gaussian shape, in contrast, is often representative of absorption lines in solids, and it describes the distribution of static dipolar fields at a nucleus in a solid.[1-3,5] The general linear-response formulation of magnetic resonance absorption which, in principle, includes both of these extreme cases was given by Kubo and Tomita,[6] who related an absorption line shape to the Fourier transform of a corresponding time autocorrelation function of the magnetization. It was subsequently shown by Lowe and Norberg,[7] using very general assumptions, that the time autocorrelation function of the transverse magnetization was equivalent to the free-induction decay (fid) or Bloch decay obtained following a 90° rf pulse. They also showed that the fid curve from a single crystal of calcium fluoride was a damped oscillatory function of time, which emphasized the non-Gaussian character of the corresponding line shape which had already been partially assessed in Van Vleck's calculation of the second and fourth moments,[8] and in the experimental work of Bruce.[9] This result stimulated further investigation into the detailed NMR line shapes produced by dipolar interactions in solids[10-18] which has led to a new formulation[19-23] of the line-shape problem that is equally valid for motionally narrowed lines in liquids.

This formulation is based on a general relation between an autocorrelation function and a certain auxiliary function, the memory function. This relationship has been established in various ways, one of which is given in a paper, subsequently referred to as I,[23] where a method due to Lado was used to relate the fid and the line shape to the memory function. The generality of this method is reflected in the fact that the natural parameters occurring in the formal solution for the line shape are the moments of the absorption line, quantities that are always defined.

The memory function enters line-shape theory as a consequence of the mathematical formalism. However, it is possible to show by qualitative arguments that its decay characteristics are related to those of a correlation function of the local field. In this respect it is similar to the correlation function occurring in the stochastic line-shape theory of Anderson and Weiss,[24] although it is more general. Thus, the memory function in solids has a decay time much greater than that associated with nonviscous liquids, as will be shown in Sec. III.

One practical application of this approach which is described in this paper is the calculation of line shapes from a knowledge of the qualitative form of the absorption line shape and its first few moments. This kind of calculation represents a compromise between a qualitative approach and a full microscopic calculation of the relevant spin correlation function. Moreover, since the lower-order moments can often be calculated exactly, they are the optimum parameters to use in adjusting a qualitative form of either a memory function or a line shape. As discussed in I and Sec. III of this paper, the form of the memory function is relatively insensitive to the form of the line shape, or, putting

it another way, the fid or line shape is less sensitive to approximations made to the memory function than to similar approximations made directly to the fid curve. Therefore, it is better to use the limited information that is available to obtain an approximate memory function, from which a fid may be calculated, than to use the same information to obtain an approximate fid curve directly. For example, it will be shown that a memory function of the same functional form can be used to calculate broad lines representative of identical spins on a rigid lattice as well as to obtain the Lorentzian line which these same spins would produce if they were in rapid, random relative motion.

II. FORMALISM FOR SYMMETRIC LINE SHAPES

As shown in I, a line shape in the linear-response approximation is always expressible as the Fourier transform of a particular autocorrelation function of the transverse magnetization. According to a theorem of Lowe and Norberg, [7] when certain high-temperature and high-field conditions are satisfied, as they usually are, this autocorrelation function is equal to the fid function. We assume in this paper that these conditions obtain. In addition, since we are only concerned with symmetric line shapes, we have specialized the results of I to this situation.

Evaluation of a time autocorrelation function may always be related to an initial value problem for the physical system of interest. In I, this problem was reformulated and reduced to a set of linear, coupled, first-order equations of motion whose formal solution was given in terms of Laplace transforms. The relation that obtains between the transforms of the fid function $G(t)$ and its associated memory function $K(t)$ is

$$\hat{G}(z)=\frac{G(0)}{z+\hat{K}(z)}. \tag{1}$$

In this notation we have, for example,

$$\hat{G}(z)=\int_0^\infty e^{-zt}G(t)\,dt. \tag{2}$$

By Laplace inversion, Eq. (1) becomes

$$\frac{dG(t)}{dt}=-\int_0^t K(t-t')G(t')\,dt'. \tag{3}$$

The memory function thus relates the rate of change of G at one time to values of G at earlier times. Its interpretation will be discussed in Sec. III. Both $G(t)$ and $K(t)$ are even functions of t which should satisfy the physical requirement that

$$G(t),\ K(t)\to 0 \ \text{ as } \ t\to\infty. \tag{4}$$

Furthermore, they have finite initial values $G(0)$ and $K(0)$. The limiting properties of the Laplace transform (2) then give the corresponding limits

$$\begin{aligned} z\hat{G}(z),\ z\hat{K}(z)&\to 0 \qquad \text{as } z\to 0\\ &\to G(0),\ K(0) \ \text{ as } z\to\infty. \end{aligned} \tag{5}$$

The decay of G and K from their initial values is generally not exponential but can nevertheless be characterized, somewhat arbitrarily, by time constants T_2^* and T_2^{**}, respectively. The relative magnitudes of these decay times as well as their absolute values are determined by the character of the spin-lattice system, as shown in Sec. III.

A line shape is given by Fourier transformation of $G(t)$, and for symmetric line shapes this relation is

$$\tilde{G}(\Delta\omega)=\frac{1}{\pi}\int_0^\infty \cos(\Delta\omega t)\,G(t)\,dt, \tag{6}$$

where $\Delta\omega=\omega-\omega_0$, ω_0 locating the center of the resonance line. In I, it was shown that (1) and (6) imply the general result

$$\tilde{G}(\Delta\omega)=\frac{G(0)}{\pi}\,\frac{K'(\Delta\omega)}{[\Delta\omega-K''(\Delta\omega)]^2+[K'(\Delta\omega)]^2}, \tag{7}$$

where

$$\begin{aligned} K'(\Delta\omega)&=\int_0^\infty \cos(\Delta\omega t)K(t)\,dt,\\ K''(\Delta\omega)&=\int_0^\infty \sin(\Delta\omega t)K(t)\,dt. \end{aligned} \tag{8}$$

Formulas (7) and (8) give an alternative approach to the calculation of the line shape once the memory function is given which may be more convenient than either (1) or (3).

The moments of $\tilde{G}$ are defined by the relation

$$M_{2n}=\frac{\int_{-\infty}^{\infty}\Delta\omega^{2n}\tilde{G}(\Delta\omega)\,d(\Delta\omega)}{\int_{-\infty}^{\infty}\tilde{G}(\Delta\omega)\,d(\Delta\omega)}. \tag{9}$$

These moments may, in principle, be used to calculate the line shape from the moment expansion. The inverse of the transformation (6) gives

$$G(t)=\int_0^\infty \cos(\Delta\omega t)\,\tilde{G}(\Delta\omega). \tag{10}$$

Consequently, assuming the existence of the moments, expansion of the cosine gives

$$\begin{aligned} G(t)&=G(0)[1-M_2t^2/2!+M_4t^4/4!-\cdots]\\ &=G(0)\sum_{n=0}^{\infty}(-1)^nM_{2n}t^{2n}/(2n)!. \end{aligned} \tag{11}$$

Although this expansion is convergent[25] it is impractical for all but the shortest times, since only the first few moments are presumed known. As application to calcium fluoride and other broad line systems has shown, however, a resummation or regrouping of its terms can give good results for most of an observed decay. [17,18] For example, the Abragam function, [3]

$$e^{-\alpha^2 t^2}\frac{\sin(\beta t)}{(\beta t)},$$

has been shown to give a good representation of the fid data from calcium fluoride when the constants α and β are matched to M_2 and M_4 using (11).[3,17] An expansion similar to (11) is obtained for $K(t)$ by combining (3) and (11). Thus we obtain

$$K(t)=K(0)[1-M_2't^2/2!+M_4't^4/4!-\cdots]$$
$$=K(0)\sum_{n=0}^{\infty}(-1)^n M_{2n}'t^{2n}/(2n)!, \quad (12)$$

where[26]

$$K(0)=M_2,\quad M_2'=M_2(M_4/M_2^2-1),$$
$$M_4'=M_2^2(M_6/M_2^3-2M_4/M_2^2+1),$$
$$M_6'=M_2^3[M_8/M_2^4-2M_6/M_2^3$$
$$+(3-M_4/M_2^2)M_4/M_2^2-1]. \quad (13)$$

This moment expansion forms the basis for obtaining approximate forms for $K(t)$ just as (11) has been used to determine approximate forms for $G(t)$.

We now consider an application of this formulation to two extreme systems, rigid-lattice solids and nonviscous liquids, in order to demonstrate the insensitivity of the memory function to the form of the line shape.

For solids such as calcium fluoride the absorption line is determined by dipolar interactions between spins, which can be regarded as residing on a rigid lattice. The second and fourth Van Vleck moments have been calculated and they give $M_4/M_2^2 \approx 2$ for all three principal orientations of the crystal axes with respect to the external field.[27] The small value of this ratio, whose minimum value is 1, is consistent with the fact that the observed line is broad and falls off rather abruptly to zero. Indeed it would seem by inspection[9] to be somewhere between a Gaussian line, $M_4/M_2^2=3$, and a rectangular line, $M_4/M_2^2=1.8$. The sixth-moment ratio would therefore be between its value for a Gaussian line, $M_6/M_2^3=15$, and that for a rectangular line, $M_6/M_2^3=3.9$. Actually this moment ratio is close to the value $M_6/M_2^3=6$ for [100] crystal orientation.[28,29] Using these ratios in (13) we obtain

$$(M_4'/M_2'^2)_{CaF_2}\approx 3.$$

Now, in nonviscous liquids, motional averaging reduces the linewidth to a small fraction of its rigid-lattice value. In this domain the Bloch equations are expected to hold, in which case the line shape is Lorentzian. A similar narrowing effect occurs on the nuclear resonance line in a crystal of paramagnetic MnF_2 because of strong exchange interactions between electron spins which average the hyperfine interaction between nuclei and electrons. The resulting exchange-narrowed line shape is also Lorentzian. Since the first few moments of this resonance line are known[30] we will use them to assess the moments associated with the memory function in the domain of extreme narrowing. For the F^{19} resonance in MnF_2, $M_4/M_2^2 \approx 0.5\times10^7$ and $M_6/M_2^3\approx 1\times10^{14}$, so that from (13) we get

$$(M_4'/M_2'^2)_{MnF_2}\approx 4.$$

The value of this ratio is typical of exchange-narrowed lines in other crystals and it is not much different from that obtained for CaF_2 even though the ratio M_4/M_2^2 has varied by a large factor. This shows that the memory function is relatively insensitive to the form of the line shape.

III. LINE-SHAPE CALCULATIONS

A. Line Shapes for a System of Spin-$\frac{1}{2}$ Particles

In this part we consider a hypothetical system of identical spin-$\frac{1}{2}$ particles experiencing their mutual dipole-dipole interactions, which may be subject to motional averaging depending on the temperature. We further consider variations in the spatial density of the nuclei, which can likewise have a significant effect on the line shape. Expressed in the language of the moments, these variations in density and temperature allow the moment ratio M_4/M_2^2 to take on its full range of values

$$1<M_4/M_2^2<\infty.$$

In spite of this wide range of values, it was shown at the end of the last section that a good approximation to the memory-function moment ratio would be $M_4'/M_2'^2=3$. This suggests that we choose a Gaussian memory function,

$$K(t)=K(0)e^{-\alpha^2 t^2}. \quad (14)$$

The parameters $K(0)$ and α are obtained from (12) and (13) as

$$K(0)=M_2,\quad \alpha^2=\tfrac{1}{2}M_2(M_4/M_2^2-1). \quad (15)$$

Having chosen this form for $K(t)$ it remains to calculate line shapes for our hypothetical system and to consider their variation with density and temperature as reflected in the variation of M_2 and M_4. The assumption (14) allows a complete line shape to be determined from only these two moments, because it fixes the relation of all the higher moments to these two lower moments.

The line-shape formula corresponding to (14) is obtained most simply from (7) since the integrals (8) may be evaluated[31] to give

$$K'(\Delta\omega)=(M_2/2\alpha)\sqrt{\pi}\,e^{-\Delta\omega^2/4\alpha^2},$$

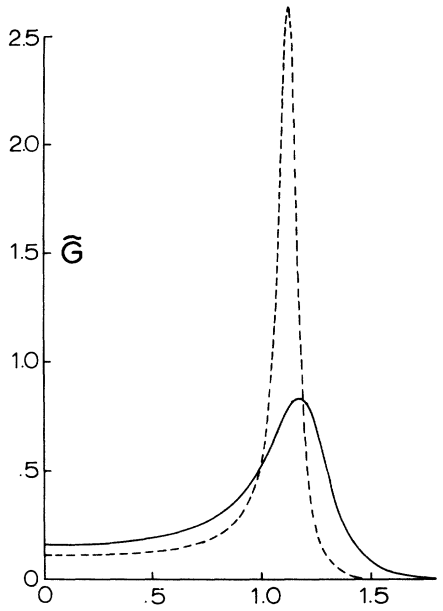

FIG. 1. Absorption line shapes for Gaussian memory function with $M_4/M_2^2=1.20$ (dashed curve) and $M_4/M_2^2=1.40$ (solid curve). $\tilde{G}(\Delta\omega)$ in units of $M_2^{1/2}$ is plotted as a function of $\Delta\omega/M_2^{1/2}$ and is normalized to unity.

$$K''(\Delta\omega)=(M_2/\alpha)(\Delta\omega/2\alpha)M(\tfrac{1}{2};\tfrac{3}{2};\Delta\omega^2/4\alpha^2)e^{-\Delta\omega^2/4\alpha^2}, \tag{16}$$

where $M(a;\ b;\ z)$ is the confluent hypergeometric function.[32] The limiting forms of K'' are

$$K''(\Delta\omega)\sim\Delta\omega \quad \text{for } |\Delta\omega|\ll 2\alpha,$$

$$K''(\Delta\omega)\sim 1/\Delta\omega \quad \text{for } |\Delta\omega|\gg 2\alpha.$$

The line shape for $|\Delta\omega|\ll 2\alpha$ is therefore a Lorentzian curve, centered at $\Delta\omega=0$, with a half-width at half-maximum, $\delta\omega$, given by

$$\delta\omega=(\pi M_2/2)^{1/2}(M_4/M_2^2-1)^{1/2}\left|M_4/M_2^2-2\right|^{-1}.$$

If the over-all shape is to be described as Lorentzian it is necessary that the condition $|\Delta\omega|\ll 2\alpha$ hold for $|\Delta\omega|\sim M_2^{1/2}$, which implies from (15) that $M_4/M_2^2\gg 1$ as expected. We then have, from (7),

$$\tilde{G}(\Delta\omega)=\frac{G(0)}{\pi}\,\frac{\delta\omega}{\Delta\omega^2+\delta\omega^2}, \tag{17}$$

$$\delta\omega=(\pi/2)^{1/2}M_2^{3/2}/M_4^{1/2},\quad M_4/M_2^2\gg 1,\quad |\Delta\omega|\lesssim M_2^{1/2}.$$

Even when (17) is valid the line shape far into the wings of the line decays as e^{-x^2}/x^2, where $x=\Delta\omega/2\alpha$ and $|\Delta\omega|\gg 2\alpha$. This asymptotic form is consistent with the existence of the moments. If the ratio M_4/M_2^2 is not large then the line shape is quite different from (17).

We have calculated a number of line shapes using (16) for different values of M_4/M_2^2 to illustrate three extreme limiting situations. These are illustrated in Figs. 1–4 and are the *pair limit*, the *solid limit*, and the *Lorentzian limit*. The line shapes in these figures are plotted as functions of $\Delta\omega/M_2^{1/2}$ for $\Delta\omega\geq 0$, and their numerical values are in units of $M_2^{-1/2}$, as they are all normalized to unity, i.e.,

$$\int_{-\infty}^{\infty}\tilde{G}(\Delta\omega)\,d(\Delta\omega)=1.$$

Each of these line shapes will be considered in turn for increasing values of the fourth-moment ratio.

For well-separated, identically oriented pairs of spin-$\frac{1}{2}$ nuclei on a rigid lattice, Van Vleck's moments[8] give

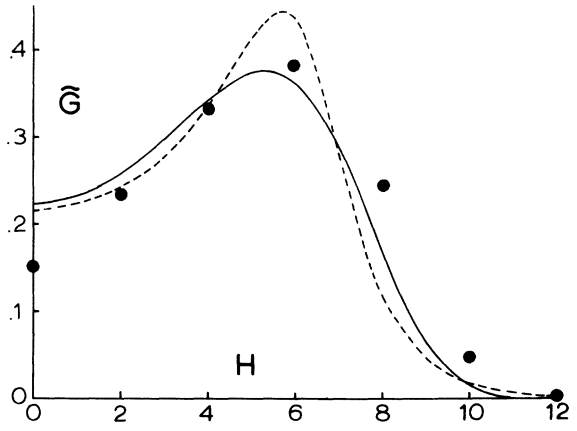

FIG. 2. Line shape for Gaussian memory function with $M_4/M_2^2=1.75$ (dashed curve) and the M_2–M_4 line shape (solid curve) compared with an experimental line shape from gypsum (circles). $\tilde{G}$ in units of $M_2^{1/2}$ is plotted as a function of ΔH in gauss.

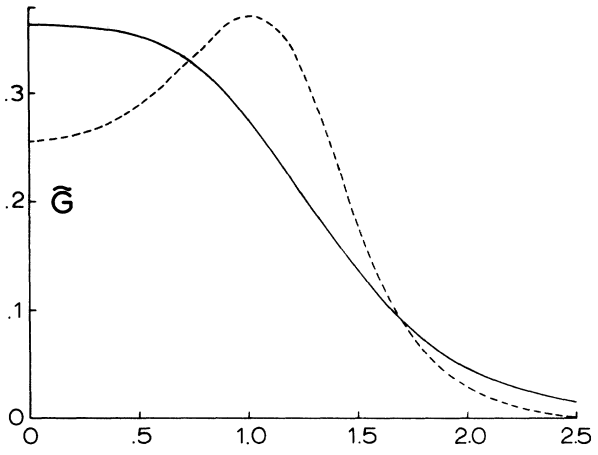

FIG. 3. Absorption line shapes for Gaussian memory function with $M_4/M_2^2=2$ (dashed curve) and $M_4/M_2^2=3$ (solid curve). $\tilde{G}(\Delta\omega)$ in units of $M_2^{1/2}$ is plotted as a function of $\Delta\omega/M_2^{1/2}$ and is normalized to unity.

$$M_2 = (9\gamma^2\mu^2/4r^6)(1-3\cos^2\theta)^2, \quad M_4/M_2^2 \gtrsim 1 .$$

In these formulas $r = |\vec{r}|$ is the distance between spins in a pair, θ is the angle between $\vec{r}$ and the external field, and the nuclear moment is $\mu = \gamma(\frac{1}{2}\hbar)$. The line shape is a pair of narrow lines on either side of $\Delta\omega = 0$.[33] In the limit $M_4/M_2^2 \to 1$ these lines approach a pair of delta functions located at[34] $\Delta\omega = \pm M_2^{1/2}$, so that $M_{2n}/(M_2)^n = 1$ for all n. Using these moments we may sum both moment series (11) and (12) to obtain $K(t) = M_2$ and $G(t) = G(0)\cos(M_2^{1/2}t)$. Actually, there will always be some residual width $\delta\omega$ to these lines which will determine the decay time T_2^* of $G(t)$ according to the usual relation $\delta\omega \approx 1/T_2^*$. The initial cosine oscillation of $G(t)$ will be damped out so that, in particular, a finite value will result for the area under this curve; i.e., $\int_0^\infty G(t)\,dt$ will be finite. From (2), this area is just $\hat{G}(0)$, which is related by (3) to the area under $K(t)$ as follows:

$$\hat{G}(0) = G(0)/\hat{K}(0) . \tag{18}$$

Since $\hat{K}(0)$ is finite, $K(t)$ must also decay to zero and its time constant will be denoted by T_2^{**}. We thus have some time τ, where $\tau < T_2^{**}$, during which

$$K(t) \approx K(0) = M_2, \quad 0 < t < \tau .$$

It follows from (3) that during this interval

$$\frac{dG(t)}{dt} \approx -M_2 \int_0^t G(t')\,dt' ,$$

and therefore

$$G(t) \approx G(0)\cos(M_2^{1/2}t), \quad 0 < t < \tau .$$

Furthermore, we have

$$M_2^{-1/2} \ll \tau \ll \delta\omega^{-1} \approx T_2^* .$$

This last condition follows from the observation that a relatively large number of oscillations of $G(t)$ must occur in the time τ if the lines are narrow so that $\delta\omega \ll M_2^{1/2}$. In this *pair limit* we have a slow decay of both $K(t)$ and $G(t)$, i.e.,

$$\delta\omega^{-1} \approx T_2^* > T_2^{**} \gg M_2^{-1/2} . \tag{19}$$

The Gaussian memory function (14) becomes a slowly decaying function when $M_4/M_2^2 \gtrsim 1$, and it is thus able to represent this situation as well as those described at the end of Sec. II. Other acceptable forms of $K(t)$ would give equally good results for short times, i.e., $t < \tau$, but they would in general produce different results for longer times. This is typical of the kind of approach we are describing. That is, given accurate values of some lower-order moments and the qualitative form of the line shape, we obtain a good approximation to the initial decay of $G(t)$. The behavior of $G(t)$ for long times, which determines the form of $\tilde{G}(\Delta\omega)$ for small $\Delta\omega$, depends strongly on the values of higher-order moments which are only approximately "evaluated" by the particular function chosen to approximate $K(t)$.

We may now calculate a detailed line shape using (16) and values of M_2 and M_4, which are presumed to be known. In the case of spin pairs on a rigid lattice there will be contributions to both moments from interpair interactions which could be calculated using Van Vleck's moment formulas. As the spin pairs are brought together the moment ratio M_4/M_2^2 increases and the effect on the line shape is shown in Fig. 1, where this ratio has been increased from 1.20 to 1.40. The location of the peaks shifts to larger values of $|\Delta\omega|$ as M_4/M_2^2 increases. This shift is accompanied by a decrease in peak height as each component line broadens in accordance with stronger interpair interactions.

As spin pairs are brought closer together these component lines continue to broaden. For example, water molecules in a crystal of gypsum produce an experimental pair line shape[35] having $M_2 = 25.4\ \mathrm{G}^2$, $M_4 = 1130\ \mathrm{G}^4$, and $M_4/M_2^2 = 1.75$[36] at that orientation for which all pairs are equivalent and maximum splitting between peaks is obtained. Using these experimental moments we have calculated a line shape from (7) and (16) which is shown in Fig. 2 together with the "M_2-M_4" line shape calculated by Powles.[36] Both shapes are qualitatively correct,[36,37] the largest discrepancy between them and experiment occurring near $\Delta\omega = 0$. The memory-function line shape is more

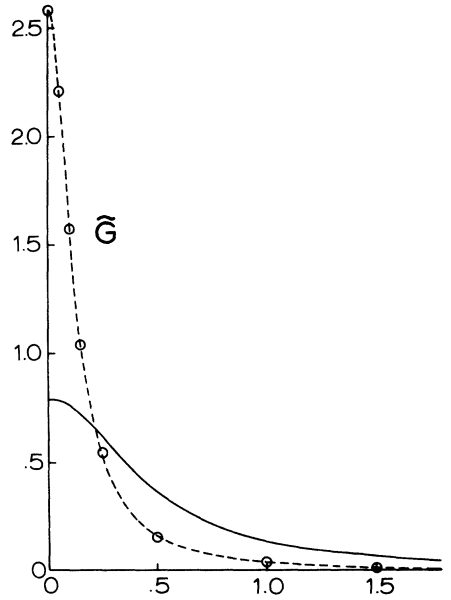

FIG. 4. Absorption line shapes for Gaussian memory function with $M_4/M_2^2 = 100$ (dashed curve) and $M_4/M_2^2 = 10$ (solid curve). $\tilde{G}(\Delta\omega)$ in units of $M_2^{1/2}$ is plotted as a function of $\Delta\omega/M_2^{1/2}$ and is normalized to unity. The circles are calculated from a Lorentzian curve.

sharply peaked than the M_2-M_4 line shape, but its peak-to-peak splitting of 11.4 G is in better agreement with the experimental value of 11.9 G[35] than the 10.6-G splitting given by the M_2-M_4 line shape. If a better approximation was desired it could be constructed using M_6. For example, the Gaussian memory function could be regarded as the first term of a cumulant expansion or a Gram-Charlier series.[17,18] The first correction term in either case could be calculated once M_6 was known. This is one way in which more details of the spin-spin interactions could be built into the line shape.

Bringing spin pairs together eventually destroys the pair concept. When the spins become more or less uniformly distributed in space the resonance line becomes a single broad line as is observed from calcium fluoride.[9] For the Gaussian memory function the transition from a pair shape to a single line occurs when $M_4/M_2^2 = 2.85$. Line shapes on either side of this transition are plotted in Fig. 3, i.e., for $M_4/M_2^2 = 2.0$ and $M_4/M_2^2 = 3.0$. The line shape for $M_4/M_2^2 = 3.0$ is not Gaussian but is more "flat topped" than a Gaussian, and it is actually more nearly like the line shapes observed from calcium fluoride than is the Gaussian shape. These flat-topped line shapes correspond by Fourier transformation to fids which oscillate as they decay to zero as is also observed. Qualitatively this situation will be described as the *solid limit* and it is characterized by

$$\delta\omega^{-1} \approx T_2^* \approx T_2^{**} \approx M_2^{-1/2} . \tag{20}$$

The transition from a rigid-lattice solid to a nonviscous liquid corresponds, in terms of the moments, to an increase in M_4/M_2^2 from about 3 to values much larger than this. The transition from $M_4/M_2^2 = 10$ to $M_4/M_2^2 = 100$, as given by the Gaussian memory function, is shown in Fig. 4. A Lorentzian line is obtained as already indicated in (17). The large value of the fourth-moment ratio also gives a rapid decay of $K(t)$ according to (14) and (15).

A more general argument, independent of the specific functional form of $K(t)$, may be given for this *Lorentzian limit*. We assume that $K(t)$ decays rapidly and monotonically to zero in a time $T_2^{**} \ll M_2^{-1/2}$, in which case it is reasonable to assume further that

$$T_2^{**} \frac{dG}{dt} \ll G \quad \text{for} \quad t \gg T_2^{**} . \tag{21}$$

It then follows from (3) that

$$\frac{dG}{dt} \approx -G(t) \int_0^t K(t-t')\,dt' \approx -G(t) \int_0^\infty K(t')\,dt' .$$

The solution is

$$G(t) \approx G(0) \exp\left[-t \int_0^\infty K(t)\,dt\right] \approx G(0) e^{-t/T_2^*}, \quad t \gg T_2^{**} . \tag{22}$$

This solution is consistent with the assumption (21) as well as the line-shape formula (17). Now, from (18), the nonoscillatory behavior of $K(t)$ and $G(t)$, and their initial values $G(0) = 1$ and $K(0) = M_2$, we have

$$T_2^* M_2^{1/2} \approx 1/T_2^{**} M_2^{1/2} ,$$

so that $T_2^* \gg M_2^{1/2}$. This also follows directly from the relation for T_2^* in (22). The *Lorentzian limit* is thus characterized by the relations

$$\delta\omega^{-1} = T_2^* \gg M_2^{-1/2} \gg T_2^{**} . \tag{23}$$

When these conditions are satisfied we obtain solutions corresponding to those given by the Bloch equations. We then have $T_2^* = T_2$ and

$$\delta\omega = \frac{1}{T_2} = \int_0^\infty K(t)\,dt . \tag{24}$$

In summary, we have shown how the insensitivity of the memory function to the form of a line shape may be exploited to obtain good qualitative agreement with certain experimental line shapes over a wide range of conditions. We have distinguished three limiting situations: the pair limit, Eq. (19); the solid limit, Eq. (20); and the Lorentzian limit, Eq. (23). In order to compare them we note that M_2 will have approximately the same numerical value in all three limits. In the pair limit the dipolar fields within the spin pair are typically about 1 G in magnitude. In the solid limit, M_2 has a somewhat larger value because more spins contribute, but it is still of the same order of magnitude. Finally in the motional narrowing transition M_2 is unchanged from its value in the solid limit. Thus the magnitude of T_2^{**} decreases as M_4/M_2^2 increases.

This decay time is related to the decay time of a local-field correlation function. First consider the Lorentzian limit. In this limit one has a correlation time τ_c given by

$$\delta\omega \approx M_2 \tau_c , \quad \tau_c M_2^{1/2} \ll 1 . \tag{25}$$

Comparison of (25) and (23) shows that $T_2^{**} \sim \tau_c$. Now τ_c is associated with fluctuations in the local field produced by lattice motion. In particular, it represents the decay time of a local-field correlation function which is of short duration owing to the rapid and random relative atomic motion. There is thus a correlation between T_2^{**} and the decay time of a local-field correlation function. This correlation also holds in the other two limiting cases. In the solid limit the decay of a local-field correlation function occurs owing to spin fluctuations which can occur in the absence of lattice fluctuations. The frequency of these fluctuations is of

TABLE I. Experimental and theoretical linewidths for F^{19} resonance in paramagnetic MnF_2, $RbMnF_3$, and $KMnF_3$.

	MnF_2	$RbMnF_3$	$KMnF_3$
Exptl.[a] (G)	37.2±1	19.7±1	19.5±1
$\delta\omega_1$ (G)	27.5	13.2	12.6
$\delta\omega_2$ (G)	34.4	16.5	15.8

[a]J. E. Gulley, D. Hone, D. J. Scalapino, and B. G. Silbernagel, Phys. Rev. B 1, 1020 (1970).

the order of $M_2^{1/2}$ and this is a measure of the duration of a local-field correlation function in this situation. By the proposed association we would have $T_2^{**} \sim M_2^{-1/2}$, which is in agreement with (20). Finally, in the pair limit one has a local field determined mainly by one neighboring spin. However, this single interaction does not produce a randomly fluctuating local field and, therefore, cannot cause relaxation. The necessary fluctuations are produced by interpair interactions which supply a spectrum of local fields much narrower than that provided in the solid limit. Thus $T_2^{**} \gg M_2^{-1/2}$ in accordance with (19).

B. Exchange Narrowing in Paramagnetic MnF_2, $RbMnF_3$, and $KMnF_3$

The F^{19} resonance line in crystals of paramagnetic MnF_2, $RbMnF_3$, and $KMnF_3$ are strongly narrowed by the electron-electron exchange interaction which averages the large hyperfine interaction between nuclei and electrons. The absorption line is Lorentzian and the experimental linewidths have been measured and are listed in Table I.[30] In addition, the moments M_2, M_4, and M_6 have been calculated.[30] Using these moments we find that for all three crystals

$$M_4/M_2^2 \approx 10^7, \quad M_4'/M_2'^2 \approx 4.$$

The large value of M_4/M_2^2 shows that extreme narrowing conditions obtain. The memory function, whatever its specific form, will have a very short value of T_2^{**} and the Lorentzian limit applies. The correct line shape is thus predicted and it remains to calculate the linewidths which may be obtained from (24) once a specific memory function has been chosen.

One possible choice would be the Gaussian memory function. Even though it has $M_4'/M_2'^2 = 3$ it should not be too bad an approximation. Using (14) and (24) we obtain the same linewidth as given by (17),

$$\delta\omega_1 = (\pi/2)^{1/2} M_2^{3/2}/M_4^{1/2}.$$

This linewidth is the same as that obtained by Gulley *et al.* using another approach.[30] It is also the linewidth obtained from the Anderson-Weiss theory[24] for a Gaussian local-field correlation function. It is compared with experimental data in Table I, where it is seen to give a value for $\delta\omega$ which is too small. A larger linewidth would be obtained by choosing a memory function which decays more slowly than the Gaussian memory function and which therefore has a larger value of the ratio $M_4'/M_2'^2$. A simple function satisfying these requirements is

$$K(t) = K(0)\,\mathrm{sech}(\alpha t) \to 2K(0)\,e^{-\alpha t}, \quad \alpha t \gg 1.$$

For this function $M_4'/M_2'^2 = 5$. The parameters are obtained using (13) and are

$$K(0) = M_2,$$

$$\alpha^2 = M_2(M_4/M_2^2 - 1).$$

From (24) we obtain

$$\delta\omega_2 = (\pi/2) M_2^{3/2}/M_4^{1/2} = 1.25\,\delta\omega_1.$$

Values of $\delta\omega_2$ are listed in Table I.

These two examples illustrate the method as applied to these crystals. A detailed analysis requires an examination of the long-time behavior of the memory function as suggested by the preceding results. Such an analysis has led to the result that at long times certain space- and time-dependent

TABLE II. Theoretical values of square root of the second moment and fourth root of the fourth moment for calcium fluoride [G. W. Canters and C. S. Johnson, Jr., J. Mag. Res. 6, 1 (1972)].

Orientation	$M_2^{1/2}$ (G)	$M_4^{1/4}$ (G)	M_4/M_2^2	$M_2^{-1/2}$ (μsec)
[100]	3.570	4.310	2.125	11.13
[111]	1.480	1.837	2.373	26.85

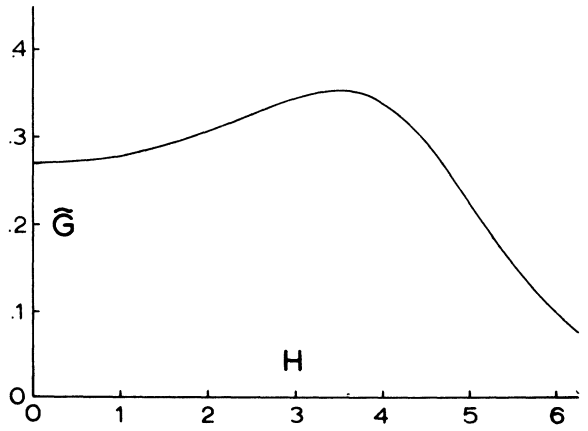

FIG. 5. Absorption line shape for Gaussian memory function with theoretical calcium fluoride second and fourth moments for [100] orientation. $\tilde{G}$ in units of $M_2^{1/2}$ is plotted as a function of ΔH in Gauss.

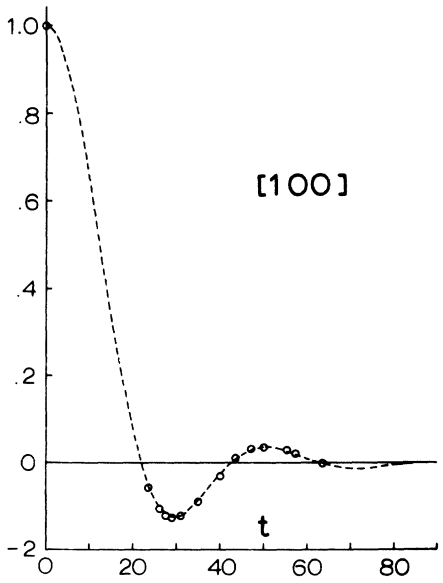

FIG. 6. fid curve calculated with Gaussian-damped Bessel-function memory function using theoretical M_2 and M_4 and adjusting M_6 and M_8 to the data of Barnaal and Lowe (open circles) for [100] orientation of calcium fluoride. $G(t)$ is normalized to unity at $t=0$ and the units of t are microseconds.

spin correlation functions in MnF_2 satisfy a diffusion equation which gives a much less rapid decay than would be suggested by the first few moments.[38] Thus, again it is seen that extrapolation of the short-time behavior of $K(t)$ to long times gives qualitative if not quantitative agreement with experiment, but it may ignore certain features that only manifest themselves at long times.

C. Calcium Fluoride Line Shapes

Nuclei in crystals of calcium fluoride can be regarded as residing on a rigid simple cubic lattice. These nuclei interact through their mutual dipole-dipole coupling, which gives a Gaussian line shape when this interaction is approximated by the classical local-field picture. The Gaussian shape is only a rough approximation to the observed line shapes, which are more nearly rectangular, particularly for [100] crystal orientation. Consequently, the associated fid curves[39] exhibit damped oscillations, these oscillations being more pronounced for [100] orientation. The moments M_2 and M_4 have been calculated from Van Vleck's formulas and are given in Table II. The difficult algebraic calculations for the sixth moment have recently been carried out[29] and even the eight-moment formula can be obtained by using special computer techniques.[40] For our purposes, however, it is sufficient to use the approximate value for the sixth moment,[28] which gives the result that

$$(M_4'/M_2'^2)_{CaF_2} \approx 3 \ . \tag{26}$$

This ratio is not sensitive to crystal orientation.

Again, in view of (26), the Gaussian memory function is a natural first choice. This assumption and the moment values in Table II completely determine a line shape which may be calculated from (7) and (16). For [100] orientation we obtain the absorption line shown in Fig. 5. This curve still exhibits some of the character of the pair limit since $M_4/M_2^2 \approx 2$; the transition to a flat-topped line occurs when $M_4/M_2^2 = 2.85$ for the Gaussian memory function. The experimental line shape [Fig. 13(a)] is not peaked. We conclude that the Gaussian memory function is not consistent with both the observed line shape and its first two even moments.[41]

One approach to obtaining a more accurate description of $K(t)$ is to use the relation (3) to calculate it from the experimental data for $G(t)$. This calculation was carried out for the [100] orientation using for $G(t)$ a fit of the Abragam function to the

TABLE III. Sixth and eighth moments expressed as ratios to second moment and related parameters determined for calcium fluoride by fit of fid curve to data of Barnaal and Lowe.

Orientation	M_6/M_2^3	M_8/M_2^4	$M_4'/M_2'^2$	ν
[100]	6.15	21.9	2.29	1.00
[111]	8.15	35.8	2.14	1.15

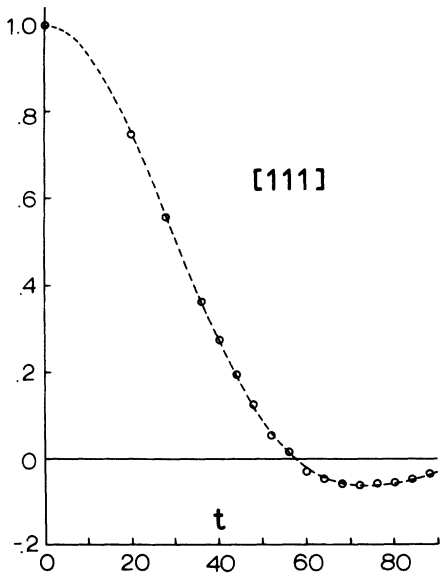

FIG. 7. fid curve calculated with Gaussian-damped Bessel-function memory function using theoretical M_2 and M_4 and adjusting M_6 and M_8 to the data of Barnaal and Lowe (open circles) for [111] orientation of calcium fluoride. $G(t)$ is normalized to unity at $t=0$ and the units of t are microseconds.

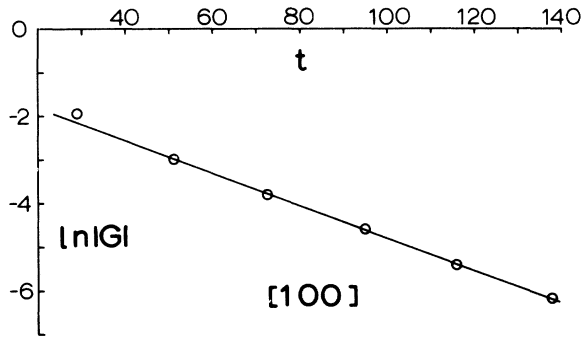

FIG. 8. Plot of the natural logarithm of the absolute value of the peaks of the normalized fid data of Lowe, Bruce, Kessemeier, and Gara (open circles) as a function of time in microseconds. A straight line is drawn through all but the first of these values.

data of Barnaal and Lowe (BL).[39] The numerical analysis was done following a method used by Berne and Harp.[42] The result is a memory function that is quite similar in shape to its corresponding fid curve except that it decays somewhat more rapidly to zero. In particular it exhibits some oscillation as it decays. For this reason we tried to fit the fid data using a memory function similar to the Abragam function. Its general form is

$$K(t) = K(0)\, e^{-\alpha^2 t^2} A_\nu (\beta t)^{-\nu} J_\nu(\beta t), \qquad A_\nu = 2^\nu \Gamma(\nu+1). \tag{27}$$

Here ν is the order of the Bessel function $J_\nu(z)$ and $\Gamma(z)$ is the gamma function. This form is suggested by the Neuman expansion theorem for decay curves.[17] The parameters are determined by the moments in (13) as follows:

$$K(0) = M_2, \quad M_2' = 2\alpha^2 + \beta^2(2\nu+2)^{-1},$$

$$M_4' = 12\alpha^4 + 6\alpha^2\beta^2(\nu+1)^{-1} + 3\beta^4[4(\nu+1)(\nu+2)]^{-1},$$

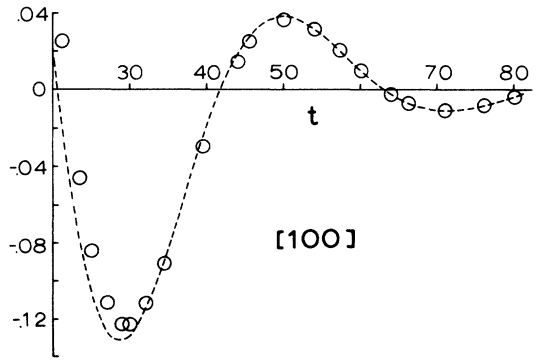

FIG. 9. fid curve of Fig. 6 (dashed curve) and the fid curve (open circles) obtained by fitting it to the long-time form suggested for calcium fluoride fid curves. $G(t)$ is normalized to unity at $t=0$ and the units of t are microseconds.

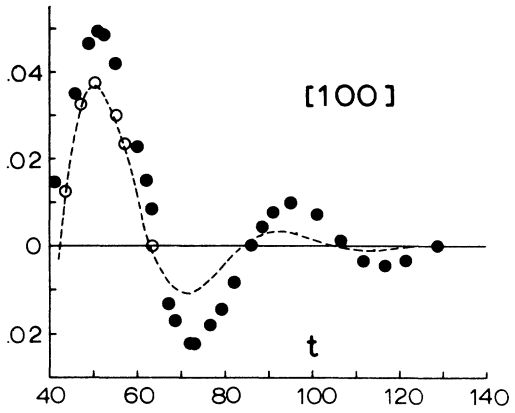

FIG. 10. fid curve of Fig. 6 at long times together with the data of Barnaal and Lowe (open circles) and of Lowe, Bruce, Kessemeier, and Gara (closed circles).

$$M_6' = 120\alpha^6 + 90\alpha^4\beta^2(\nu+1)^{-1} + 45\alpha^2\beta^4[2(\nu+1)(\nu+2)]^{-1} + 15\beta^6[8(\nu+1)(\nu+2)(\nu+3)]^{-1}. \tag{28}$$

These parameters were obtained using theoretical values of M_2 and M_4 (Table II) and by adjusting M_6 and M_8 until optimum agreement was obtained with the data of BL.

The line-shape formulas (8) cannot be evaluated analytically for the function (26). We therefore used (3) to calculate $G(t)$ directly from $K(t)$. The numerical method[42] gave $G(t)$ at 600 time points whose spacing was $0.025 M_2^{-1/2}$. A line shape was calculated from (6) using a modification of Filon's rule.[43] This procedure was tested using the function given for this purpose by Berne and Harp.[42] Accurate values of G were obtained for both long and short times. As a second independent test the method just described was used to calculate a line shape for the Gaussian memory function which was then compared with that curve obtained directly from (7) and (16). These results were also consistent.

Calculated fid curves for [100] and [111] orientations, subsequently referred to as G_{cal}, are shown in Figs. 6 and 7 together with the data of BL to which they were fitted. Moment values and related parameters obtained by this procedure are given in Table III. They are consistent with those calculated from Bruce's data and Abragam's function.[3]

TABLE IV. Parameters in the long-time form of calcium fluoride fid curve.

Orientation	a (cal.) (μsec^{-1})	a (exptl.) (μsec^{-1})	π/b (cal.) (μsec)	π/b (exptl.) (μsec)
[100]	0.058	0.037	21.2	21.8
[111]	0.034	0.022	48	44

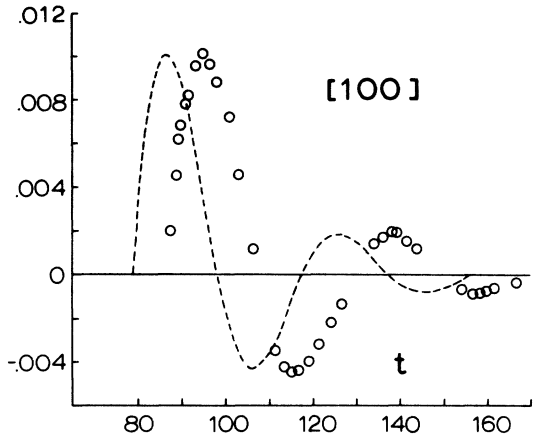

FIG. 11. Long-time fid curve calculated with Gaussian-damped Bessel-function memory function using moment parameters somewhat different from those used to obtain Figs. 6 and 7. The data of Lowe, Bruce, Kessemeier, and Gara is also shown (open circles). $G(t)$ is normalized to unity at $t=0$ and the units of t are microseconds.

Measurements on CaF_2 made at low temperatures by Lowe, Bruce, Kessemeier, and Gara (LBKG)[44] have shown that the long-time portion of a decay curve has a form qualitatively different from that obtained at short times, i.e., for the interval of time covered by the data of BL, Figs. 6 and 7. A good approximation for short times is obtained by using the Abragam function

$$G(t) \approx e^{-\alpha^2 t^2} \frac{\sin \beta t}{\beta t}, \quad t \lesssim T_2^* . \tag{29}$$

At longer times, however, the data of LBKG shows that[45]

$$G(t) \approx d e^{-at} \cos(bt + c), \quad t > T_2^* . \tag{30}$$

For example, in Fig. 8 is plotted values of $\ln|G_p|$, where G_p is the experimental value of the fid curve at one of its peaks. This curve is a straight line whose slope gives a value for the parameter a in (29). The parameter b is obtained from the period-

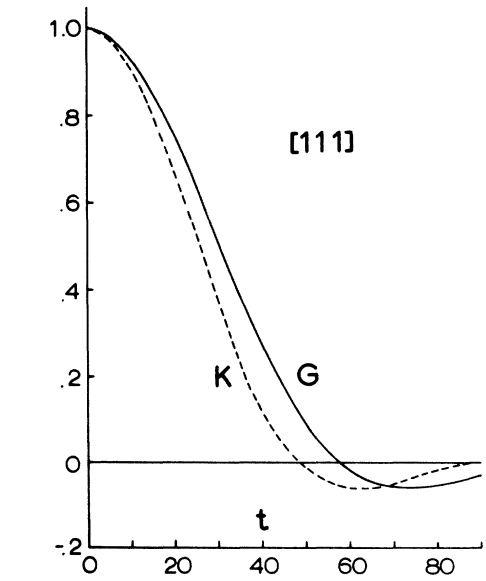

FIG. 12. fid curve of Fig. 7 (solid curve) and its associated memory function (dashed curve). $G(t)$ is normalized to unity at $t=0$ and $K(t)$ is given in units of M_2. The units time are microseconds.

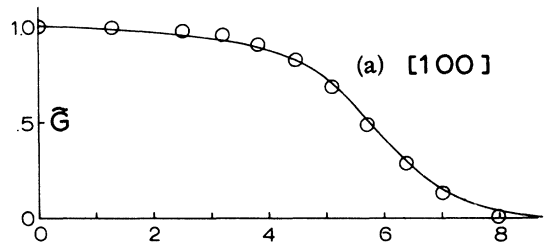

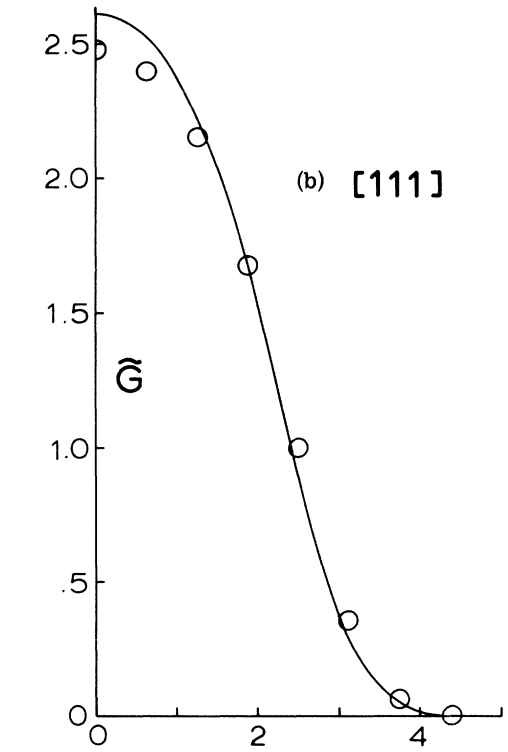

FIG. 13. (a) Calcium fluoride absorption line shape for [100] orientation calculated as the Fourier transform of the fid curve in Fig. 6 and Bruce's data (circles). Both line shapes were separately normalized to the same area and they are plotted as a function of ΔH expressed in gauss. (b) Calcuim fluoride absorption line shape for [111] orientation calculated as the Fourier transform of the fid curve in Fig. 7 and Bruce's data (circles). Both line shapes were separately normalized to the same area and they are plotted as a function of ΔH expressed in gauss.

icity exhibited by the data. Results of this data analysis for [100] and [111] orientations are given in Table IV.

Now, in contrast to the Abragam function (28), G_{cal} exhibits the correct qualitative long-time behavior. For example, for [100] orientation we obtain

$$G_{cal} \approx 0.75 e^{-0.058t} \cos(\pi t/21.2 - 0.47\pi), \quad t \gtrsim 30\ \mu\text{sec}. \tag{31}$$

This function is plotted in Fig. 9 together with points representing G_{cal}. The onset of this asymptotic behavior occurs at $t \approx 30$ μsec for [100] orientation. The a and b parameters in (30) were obtained in the same fashion as the experimental a and b parameters.[48] Both are listed in Table IV. Comparison of these results show that the calculated fid curve decays too rapidly. This is also shown in Fig. 10, where G_{cal} is plotted together with the data of BL and LBKG. Even though a(cal.) is too large there is good agreement between b(cal.) and b(exptl.). Since b represents some average beat frequency which also occurs in (28) this is perhaps not surprising. If the moments are varied somewhat G_{cal} can be forced to give a smaller decay constant as shown in Fig. 11. A necessary consequence of this, however, is that b(cal.) now becomes too large and the agreement with the data of BL becomes less satisfactory.

In Fig. 12 is shown the [111] memory function and its associated fid curve, both normalized to unity for purposes of comparison. These curves are quite similar, the main difference being that $K(t)$ decays somewhat more rapidly than $G(t)$.

In Figs. 13(a) and 13(b) are plotted the [100] and [111] line shapes obtained by Fourier transformation of G_{cal}. They are compared to Bruce's data. The largest difference between his data and these line shapes occurs for the [111] orientation. The $\tilde{G}_{cal}$ line shape is more sharply peaked than the experimental one, which may be partly due to a small misalignment of his crystal. Calcium fluoride line shapes are most sensitive to crystal alignment near [111] orientation, where any deviation from this alignment produces a broadening of the line. This interpretation is consistent with the fact that the Fourier transform of Bruce's data decays to zero more rapidly than the [111] data of BL.

[1] N. Bloembergen, E. M. Purcell, and R. V. Pound, Phys. Rev. **73**, 679 (1948).
[2] G. E. Pake and E. M. Purcell, Phys. Rev. **74**, 1884 (1948).
[3] A. Abragam, *The Principles of Nuclear Magnetism* (Oxford U. P., London, 1961), Chaps. 4 and 10.
[4] F. Bloch, Phys. Rev. **70**, 460 (1946). See also Ref. 3.
[5] G. W. Parker, Am. J. Phys. **38**, 1432 (1970).
[6] R. Kubo and K. Tomita, J. Phys. Soc. Jap. **9**, 888 (1954).
[7] I. J. Lowe and R. E. Norberg, Phys. Rev. **107**, 46 (1957).
[8] J. H. Van Vleck, Phys. Rev. **74**, 1148 (1948).
[9] C. R. Bruce, Phys. Rev. **107**, 43 (1957).
[10] S. Gade and I. J. Lowe, Phys. Rev. **148**, 382 (1966).
[11] S. Clough and I. R. McDonald, Proc. Phys. Soc. Lond. **86**, 833 (1965).
[12] M. Lee, D. Tse, W. I. Goldburg, and I. J. Lowe, Phys. Rev. **158**, 246 (1967).
[13] W. A. B. Evans and J. G. Powles, Phys. Lett. A **24**, 218 (1968).
[14] D. Demco, Phys. Lett. A **27**, 702 (1968).
[15] R. E. Fornes, G. W. Parker, and J. D. Memory, Phys. Rev. B **1**, 4228 (1970).
[16] H. Betsuyaki, Phys. Rev. Lett. **24**, 934 (1970).
[17] G. W. Parker, Phys. Rev. B **2**, 2453 (1970).
[18] B. T. Gravely and J. D. Memory, Phys. Rev. B **3**, 3426 (1971).
[19] P. Resibois, P. Borckmans, and D. Walgraef, Phys. Rev. Lett. **17**, 1290 (1966).
[20] P. Borckmans and D. Walgraef, Phys. Rev. **167**, 282 (1968).
[21] P. Borckmans and D. Walgraef, Phys. Rev. Lett. **21**, 1516 (1968).
[22] J. A. Tjon, Phys. Rev. **143**, 259 (1966).
[23] F. Lado, J. D. Memory, and G. W. Parker, Phys. Rev. B **4**, 1406 (1971).
[24] P. W. Anderson and P. R. Weiss, Rev. Mod. Phys. **25**, 269 (1953); P. W. Anderson, J. Phys. Soc. Jap. **9**, 316 (1954); see also Ref. 3; and R. Kubo, in *Fluctuation Relaxation and Resonance in Magnetic Systems*, edited by D. ter Haar (Oliver and Boyd, Edinburgh and London, 1962).
[25] This would seem to be the case of calcium fluoride on the basis of experimental or theoretical moment values and from comparison of the Gaussian shape and the experimentally observed line shapes which are distinctly more flat topped.
[26] The primed moments are associated with the memory function in this paper; in I they denoted the central moments of a symmetric line.
[27] G. W. Canters and C. S. Johnson, Jr., J. Mag. Res. **6**, 1 (1972).
[28] Unpublished calculations by S. R. Long based on the sixth-moment formula obtained by Cheng and Memory, Ref. 29, have shown that $M_6/M_2^3 \approx 6$ for the [100] orientation.
[29] E. T. Cheng and J. D. Memory, Phys. Rev. B **6**, 1714 (1972); W. F. Wurzbach and S. Gade, Phys. Rev. B **6**, 1724 (1972); W. F. Wurzbach, S. Gade, E. T. Cheng, and J. D. Memory, Phys. Rev. B **7**, 2209 (1973).
[30] J. E. Gulley, D. Hone, D. J. Scalapino, and B. G. Silbernagel, Phys. Rev. B **1**, 1020 (1970).
[31] *Tables of Integral Transforms*, The Bateman Manuscript Project, edited by A. Erdelyi (McGraw-Hill, New York, 1954), pp. 15 and 73.
[32] *Handbook of Mathematical Functions*, edited by M. Abramowitz and I. A. Stegun (Dover, New York, 1965), Chap. 13.
[33] G. E. Pake, J. Chem. Phys. **16**, 327 (1948).
[34] The peak-to-peak spacing is $2M_2^{1/2}$. Using the expression for M_2 gives the Pake splitting (Ref. 33).
[35] B. Pederson and D. F. Holcomb, J. Chem. Phys. **38**, 61 (1963).
[36] J. G. Powles and B. Carazza, *Proceedings of the International Conference on Magnetic Resonance, Melbourne, 1969* (Plenum, New York, 1970).
[37] D. F. Holcomb and B. Pedersen, J. Chem. Phys. **38**, 54 (1963).
[38] See, for example, Ref. 30.
[39] D. E. Barnaal and I. J. Lowe, Phys. Rev. **148**, 328 (1966).
[40] S. J. K. Jensen and E. K. Hansen, Phys. Rev. B 7, 2910 (1973).
[41] If we are willing to regard M_2 and M_4 as adjustable parameters we could obtain a reasonably good fit to the data

without changing their values too much.

[42]B. J. Berne and G. D. Harp, Adv. Chem. Phys. **17**, 63 (1970), Appendix B.

[43]L. N. G. Filon, Proc. R. Soc. Edinb. A **49**, 38 (1928). See also, Ref. 33, p. 890. Another method has been described by F. Lado, J. Comput. Phys. **8**, 417 (1971).

[44]Unpublished data. We are indebted to Professor R. E. Norberg for sending copies of this data.

[45]This form is not a consequence of nuclear spin diffusion since this phenomena occurs for times $t \gg T_2^*$ in contrast to electron spin diffusion, in say MnF_2, which is important for times $t \lesssim T_2^*$. The spin-diffusion constant varies approximately as the square of the gyromagnetic ratio [see, for example, I. J. Lowe and S. Gade, Phys. Rev. **156**, 817 (1967)], which greatly reduces its value in a nuclear-spin system relative to its value in an electron-spin system.

[46]Determination of an approximate fid curve at long times from some approximation to $K(t)$ was discussed in I. The behavior of $G(t)$ at long times is associated with the form of $\hat{G}(z)$ near $z = 0$ [see Eq. (4)]. Since $\hat{G}$ is related by (1) to $\hat{K}$, the small-z form of this latter function is required. Alternatively, if the complete form of $\hat{K}$ is known, the zeros of $z + \hat{K}(z)$ would be calculated since the root having the smallest real part then determines the associated decay constant at long times (the imaginary part if nonzero would cause oscillations). Neither of these methods were employed for the memory function (26) due to the complexity of the resulting integrals.